Energy fluctuations in a biharmonically driven nonlinear system

NAVINDER SINGH, SOURABH LAHIRI* and A M JAYANNAVAR

Institute of Physics, Sachivalaya Marg, Bhubaneswar 751 005, India
*Corresponding author. E-mail: lahiri@iopb.res.in

Abstract. We study the fluctuations of work done and dissipated heat of a Brownian particle in a symmetric double well system. The system is driven by two periodic input signals that rock the potential simultaneously. Confinement in one preferred well can be achieved by modulating the relative phase between the drives. We show that in the presence of pumping the stochastic resonance signal is enhanced when analysed in terms of the average work done on the system per cycle. This is in contrast with the case when pumping is achieved by applying an external static bias, which degrades resonance. We analyse the nature of work and heat fluctuations and show that the steady state fluctuation theorem holds in this system.

1. Introduction

A number of important results have been obtained over the last two decades on the statistical properties of fluctuations in physical quantities in nonequilibrium processes. These are referred to as fluctuation theorems (FTs) [1–17]. They allow extension of thermodynamic concepts to small systems [1]. The fluctuation theorems reveal rigorous relations for the properties of distribution functions of physical variables such as work done, dissipated heat or entropy production for systems driven far away from equilibrium, independent of the nature of driving. They are not restricted to the linear response regime, thus allowing us to obtain results by generalizing Onsager reciprocity relations to the nonlinear response coefficients in nonequilibrium state. From these theorems, corollaries such as the statistical derivation of the second law, can be established. There are different fluctuation theorems, depending on the physical quantities they relate to and on the state of the system they refer to. These theorems are useful to probe nonequilibrium states in nanophysics and biology. Hence they are anticipated to play an important role in the design of nanodevices and engines (molecular motors) at nanoscales. The

Navinder Singh, Sourabh Lahiri and A M Jayannavar

distributions of heat and work in relation to FTs have been experimentally studied for a few Brownian systems [18–23].

In recent theoretical [24,25] and experimental [26] studies, the distributions of dissipated heat and work done on the system have been explored in a system exhibiting stochastic resonance [24,25]. The steady state fluctuation theorem (SSFT) (as elaborated upon in §3.6) holds in this system. Exploring the FTs in nonlinear systems by changing the symmetry of the driving force cycle has been suggested in ref. [26]. To this end, we study the dynamics of a particle in a symmetric double well potential which is in contact with a thermal bath at temperature T. This system exhibits stochastic resonance (SR) under subthreshold external AC drive [27]. The fundamental periodic component of the system response (i.e., the amplitude of the feeble input at the same frequency) can be amplified by the assistance of noise. It is reflected as a peak in the output signal-to-noise ratio as a function of noise strength. This peak occurs when the noise-induced switching rate in the system matches the forcing frequency. This optimization or synchronization condition is achieved by tuning the noise intensity. This phenomenon is known as stochastic resonance [27,28]. Here noise plays a constructive role as opposed to our conventional wisdom that the presence of noise degrades the signal. This is due to a cooperative interplay between the system nonlinearity and input signal in addition to the noise. Because of its generic nature, this phenomenon boasts applications in almost all areas of natural science [28]. To characterize this resonance phenomenon, several different quantifiers have been introduced in the literature [28–35]. One of the quantifiers, namely, the input energy of the system or the work done on the system per cycle is known to characterize SR as a bona fide resonance [24,25,34,35]. In this case, the resonance can be shown to occur both as a function of noise strength and driving frequency.

It is known that static asymmetry in the bistable potential weakens the magnitude of the SR effect [25,28]. Static tilt in the potential makes one potential well more stable than the other leading to more particle localization or pumping in one well (lower well) compared to the other. Moreover, due to asymmetry in the potential, escape rate of a particle from higher to lower well will be different from lower to higher well. These two different rates make synchronization difficult between the signal and the dynamics of the particle hopping, since the driving frequency cannot match both these hopping rates simultaneously.

In the present work, we study the SR for a particle in a symmetric double well potential, driven simultaneously by two periodic signals of frequencies ω and 2ω with a relative phase difference ϕ between them. Such a force averaged over a period does not lead to a net bias and yet particle is preferentially pumped into one well depending on phase difference ϕ and other physical parameters [36–42]. This phenomenon is known as harmonic mixing [36–39]. Due to this statistical confinement of the particle, similar to the case of static tilt [28,43], we expect to observe a reduced SR signal in this system. However, contrary to this expectation, we show that the resonance signal is enhanced in the presence of the biharmonic drive at frequency 2ω when analysed in terms of the input energy (or the work done) as a quantifier of SR. Using stochastic energetics [13,44,45] we also study the nature of fluctuations in the work done, dissipated heat and internal energy across SR. In some range of parameters, the nature of hysteresis loops is analysed. We

show that the SSFT holds for work done over a long time interval. The modified SSFT for heat is also studied in this system.

2. The model: Brownian particle in a rocked double well potential

We consider the stochastic dynamics of a Brownian particle in a double-well potential $V(x) = -\frac{x^2}{2} + \frac{x^4}{4}$, rocked by a weak biharmonic (time-asymmetric) external field $F(t) = A\cos(\omega t) + B\cos(2wt + \phi)$. The potential $V(x)$ has two minima at $x = \pm 1$, separated by a central (at $x = 0$) potential barrier of height $\Delta V = 0.25$. The overdamped Langevin dynamics is given by [46]

$$\gamma \frac{\mathrm{d}x}{\mathrm{d}t} = -\frac{\partial U(x,t)}{\partial x} + \xi(t), \tag{1}$$

where $U(x,t) = V(x) - xF(t)$, γ is the friction coefficient, $\xi(t)$ is the Gaussian white noise with the properties

$$\langle \xi(t) \rangle = 0,$$
$$\langle \xi(t)\xi(t') \rangle = 2D\delta(t - t'), \tag{2}$$

where $D = \gamma k_{\mathrm{B}}T$. The thermodynamic work done by an external drive over a period $\tau_\omega (= 2\pi/\omega)$ is given by [13,44,45]

$$W_p = \int_{t_0}^{t_0+\tau_\omega} \frac{\partial U(x,t)}{\partial t} \mathrm{d}t$$
$$= \int_{t_0}^{t_0+\tau_\omega} x(t)[A\omega\sin\omega t + 2B\omega\sin(2\omega t + \phi)]\mathrm{d}t. \tag{3}$$

This work (or input energy) over a period equals the change in the internal energy $\Delta U_p = U(x(t_0 + \tau_\omega), t_0 + \tau_\omega) - U(x(t_0), t_0)$ plus the heat dissipated over a period Q_p, i.e.,

$$W_p = \Delta U_p + Q_p. \tag{4}$$

The above equation is the statement of the first law of thermodynamics and can readily be obtained using stochastic energetics [44]. Since $x(t)$ is a stochastic variable, it follows from eqs (3) and (4) that $W_p, \Delta U_p$ and Q_p are random variables when evaluated over different periods and realizations of $x(t)$. The above model is solved numerically by using Heun's method [47] (all the physical quantities are in dimensionless units). We have ignored the initial transient regime up to time t_0 and evaluated W_p, Q_p, and ΔU_p over many cycles ($\sim 10^5$) of a single long trajectory of the particle.

3. Results and discussions

3.1 *SR as a function of noise strength*

In figure 1, we have plotted the average work done over a single period $\langle W_p \rangle$ in the time asymptotic regime as a function of noise strength D for different values

Navinder Singh, Sourabh Lahiri and A M Jayannavar
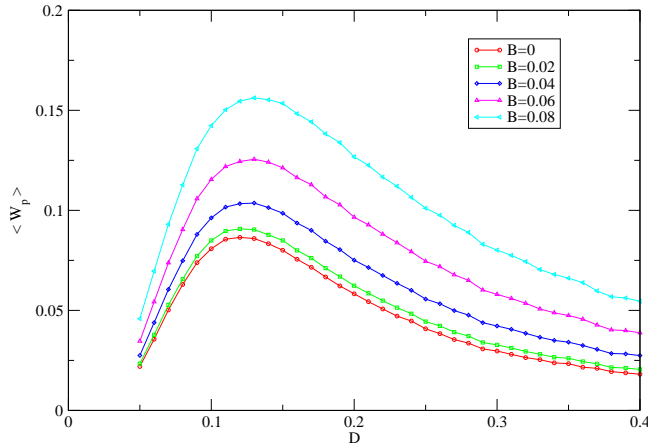
Figure 1. The input energy $\langle W_p \rangle$ as a function of D for different values of the strength of second harmonic (B). The parameters are: $\omega = 0.1, A = 0.1$ and $\phi = 0$.

of biharmonic drive strength B (for $A = 0.1$). Phase difference is taken to be zero. Other parameters are mentioned in the figure captions. For the case of $B = 0$ we have reproduced earlier results [24,25,34,35]. The average input energy ($\langle W_p \rangle$) shows a peak signifying stochastic resonance (SR) as discussed extensively in earlier literature [24,25,34,35]. The quantity $\langle W_p \rangle$ can also be identified as the average dissipated heat or hysteresis loss into the bath in a time periodic steady state. This follows from eq. (4) by noting that the internal energy being a state variable, ΔU_p averaged over a period is identically equal to zero. As we increase B, $\langle W_p \rangle$ increases for a fixed value of D. Moreover, for different values of B, the system exhibits SR as a function of noise strength. The system in a steady state absorbs energy from the external drive and the same is dissipated as heat into the surrounding medium. Hence, it is expected that at the resonance the system will absorb maximum energy from the external drive. The input energy curves for higher values of B lie above those for the lower values of B. The graph for $B = 0$ matches with the earlier known results [25,34,35], and the peak position shifts towards higher values of D. It is evident from the figure that in the presence of biharmonic drive, enhancement of SR signal occurs even though there is more statistical confinement of the particle (as B increases) in one well as shown in figure 2. In this figure we have plotted average position ($\langle x \rangle$) over period in the time asymptotic regime as a function of B for fixed $D = 0.05$. The value of $\langle x \rangle$ not being zero signifies selective pumping or localization of particle from one well to another in the presence of biharmonic drive. Correspondingly, the probability density distribution of the particle averaged over a period shows a marked asymmetry even though the potential $V(x)$ is symmetric [38]. In the absence of second harmonic component i.e., $B = 0$, $\langle x \rangle = 0$ as expected. The pumping is very significant at low values of temperature. As we increase temperature, the effective pumping reduces. Around and beyond SR, pumping is quite small as shown in the inset of figure 2.
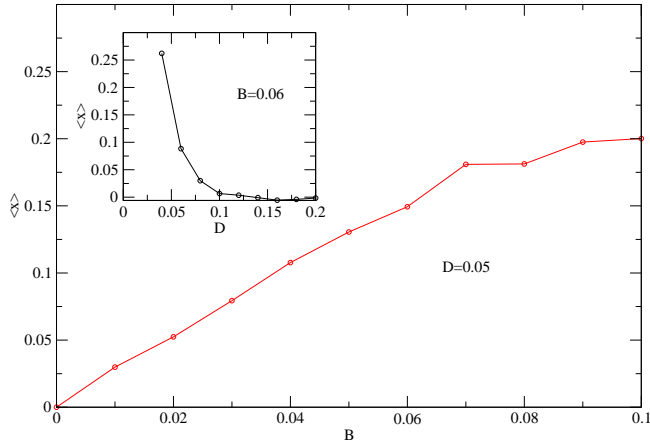
Figure 2. Particle mean position $\langle x \rangle$ as a function of B for $D = 0.05$. In the inset we have plotted $\langle x \rangle$ as a function of D. Other parameters are: $B = 0.06, A = 0.1$ and $\omega = 0.1$.
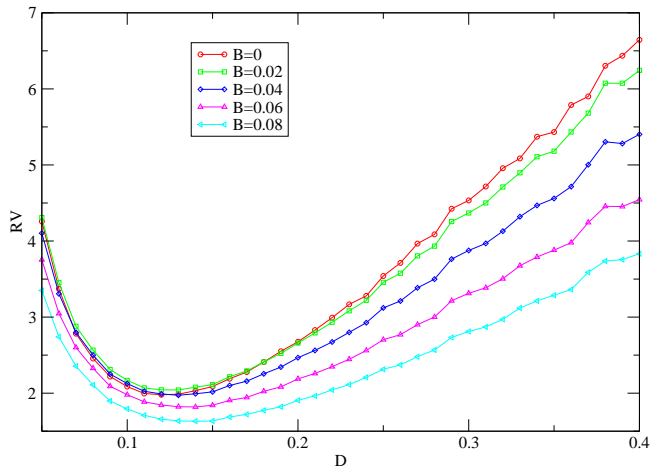
Figure 3. Relative variance (RV) of input energy vs. D for different values of B. Other parameters are same as in figure 1.

Stochastic resonance being a synchronization phenomenon [30,33] it is expected that particle hopping dynamics between the wells get synchronized with the input signal. We find that the relative variance (RV) in physical quantities such as work $\left[= \frac{\sqrt{\langle W_p^2 \rangle - \langle W_p \rangle^2}}{\langle W_p \rangle} \right]$ and heat $\left[= \frac{\sqrt{\langle Q_p^2 \rangle - \langle Q_p \rangle^2}}{\langle Q_p \rangle} \right]$ also show minima at SR [24–26].

In figure 3 we have plotted relative variance (RV) as a function of D for various values of B. The parameters used are the same as in figure 1. For a given value of B, RV shows a minimum around the same value of D at which $\langle W_p \rangle$ exhibits a maximum. As the amplitude of the biharmonic drive B increases, RV curves shift downwards. Higher the value of B, the lower is the value of RV at the resonance.

Navinder Singh, Sourabh Lahiri and A M Jayannavar
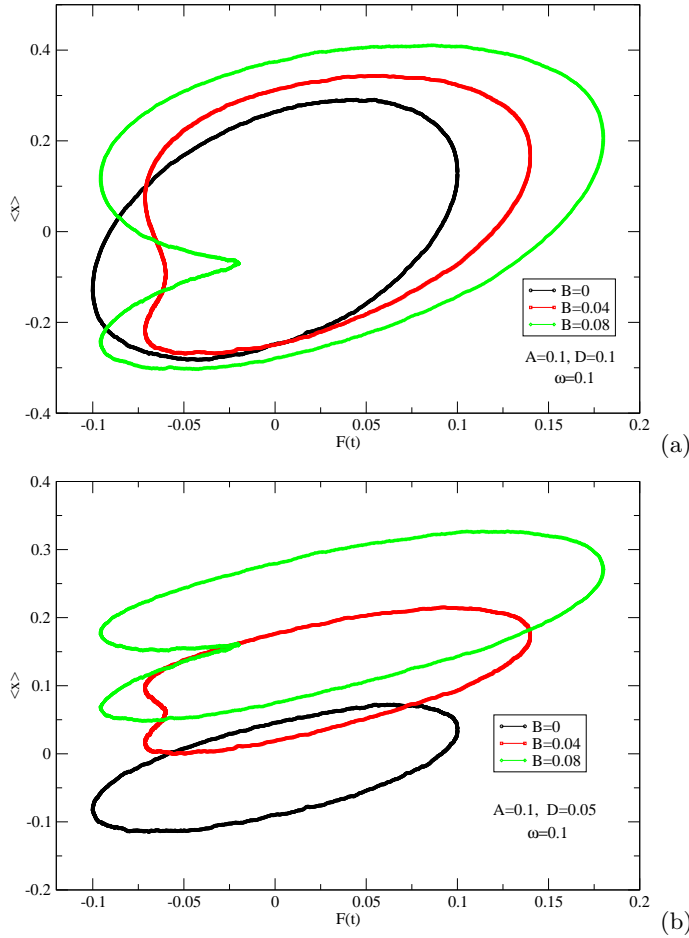
Figure 4. (**a**) Hysteresis loops ($\langle x \rangle$) vs. F for different values of B for $D = 0.1$. Other parameters are same as in figure 1. (**b**) Hysteresis loops for different values of B for $D = 0.05$.

These results are consistent with figure 1. In the parameter regime that we have considered, RV is larger than one, i.e., variance in work is large compared to the mean. Hence in this regime, one should analyse full probability distribution as opposed to moments to get better understanding of the phenomenon.

Increasing the amplitude of biharmonic drive leads to more statistical confinement of particles (figure 2). This must be reflected in the nature of hysteresis loops [33,40]. More the pumping, more is the asymmetry in the hysteresis loops, as can be seen in figures 4a and b. In these figures hysteresis loops are plotted for different values of D and B. The pumping of the particles also gets reflected in the shifting of figures in the vertical upward direction (as $\langle x \rangle > 0$). For the case when $B = 0$, there will be no pumping and as expected the loop is symmetric.
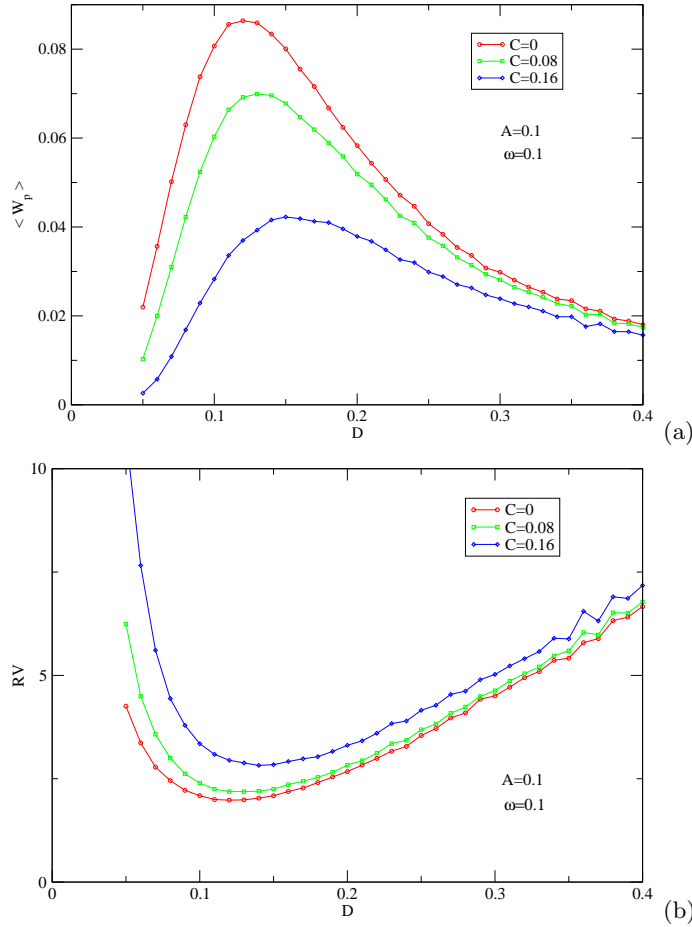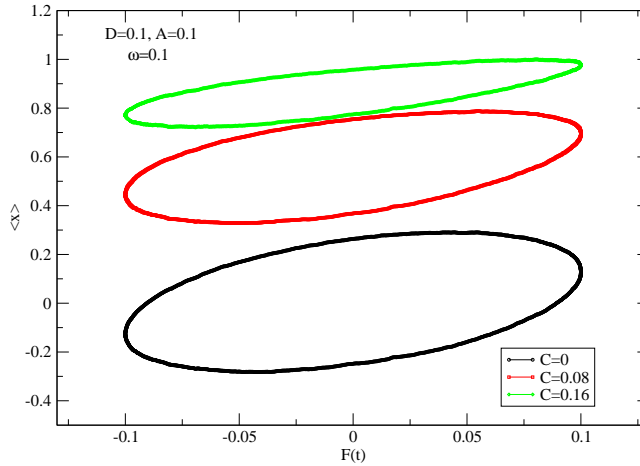
Figure 5. (**a**) Plots of $\langle W_p \rangle$ as a function of D for different values of the static tilt c. (**b**) Corresponding plots of relative variance of W_p as a function of D. Fixed parameters are mentioned in the graphs.

3.2 *SR in the presence of static tilt*

Particle pumping in a preferential well can also be induced by applying a static tilt to the otherwise symmetric double well potential. For this we take the potential to be $V_1(x) = -\frac{x^2}{2} + \frac{x^4}{4} - cx$. Depending on the value of c, the potential $V_1(x)$ becomes asymmetric and obviously more pumping results in the lower potential well. When this system is driven by external AC force $A \cos \omega t$ we show that SR signal weakens. Figure 5a shows the average input energy as a function of D for various values of c. From this, we notice that the input energy curves for higher values of c are below those with lower values of c (other parameters being fixed). As c increases, SR peak becomes broadened and shifts towards higher values of D. We thus observe that in the presence of pumping induced by static tilt, SR weakens as

Figure 6. Plots showing hysteresis loops for different values of static tilt c. Fixed parameters are: $D = 0.1, A = 0.1$ and $\omega = 0.1$.

mentioned in the Introduction. This is also corroborated by the nature of relative work fluctuations as a function of D (figure 5b). From this figure we note that as we increase c, RV increases for a given value of D. The magnitude of the RV at the minimum becomes larger as we increase c. This implies degradation of SR signal in the presence of particle pumping induced by a static tilt. The pumping due to static tilt makes the hysteresis loops asymmetric (figure 6). By increasing c more pumping is achieved and this is reflected in the vertical shift of hysteresis loops. Thus from the above figures and discussions, we conclude that in the presence of biharmonic drive, SR increases while in the presence of static tilt, SR weakens.

3.3 *SR as a function of driving frequency*

In figure 7a, we have plotted average input energy as a function of ω for various values of B. Once again we notice that SR signal even for this case is increased as we increase the biharmonic component B. Each curve exhibits a peak as a function of ω, thus establishing SR as a bona fide resonance. The peak shifts to the lower values of ω as we increase B. This is consistent with the fact that peaks in figure 1 shift towards larger values of D as we increase B. This is a requirement for the time-scale matching between D and ω. Since increase in B slows down the effective time-averaged hopping rates between the wells, higher D is required to achieve resonance. This lowering of effective escape rate at a given D in turn implies decrease in the resonant frequency. The enhancement of SR signal in the presence of B can be inferred from figure 7b where we have plotted relative variance across the SR as a function of ω for various values of B. Lower values of relative variance across the SR for larger values of B are suggestive of the fact that SR is enhanced in the presence of biharmonic drive, consistent with the conclusions of figure 1.
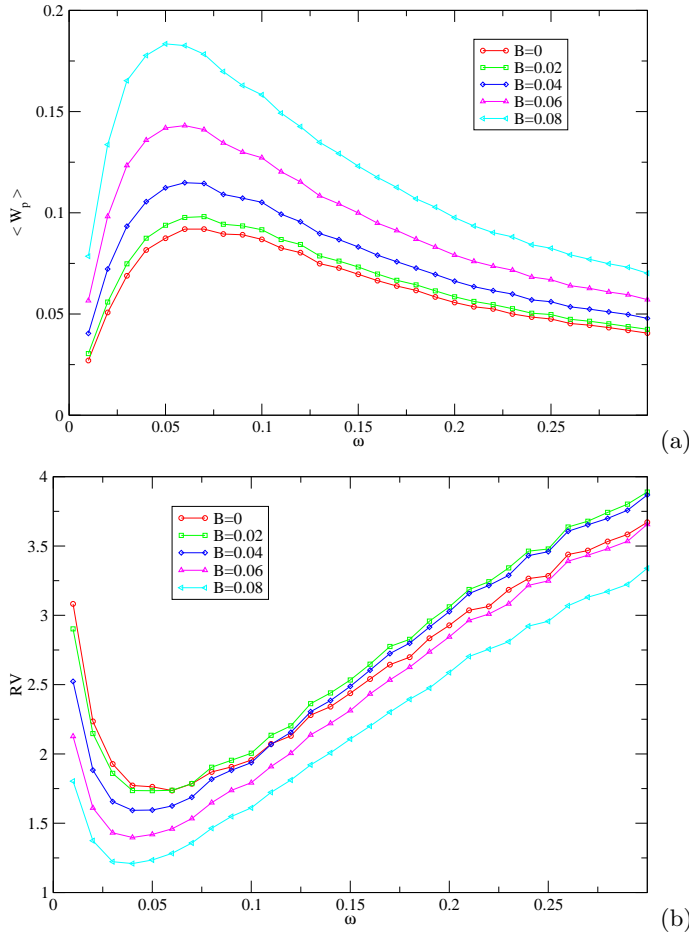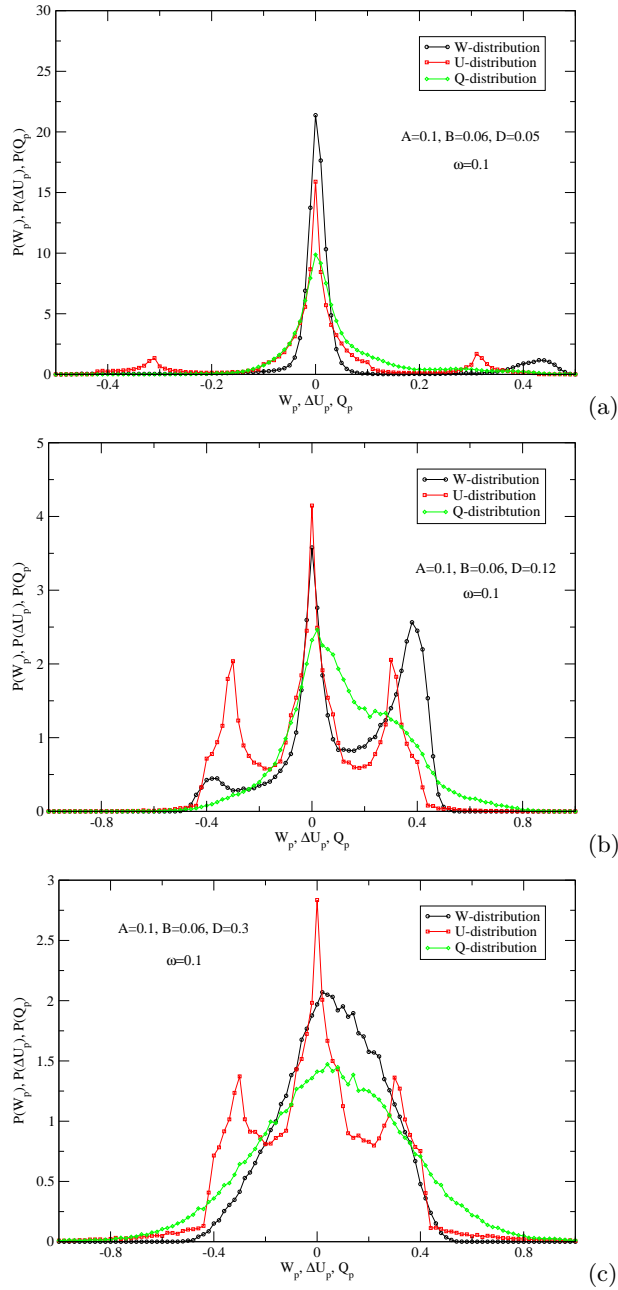
Figure 7. (**a**) The average input energy per period $\langle W_p \rangle$ as a function of frequency ω. (**b**) Relative variance (RV) of input energy vs. frequency ω for different values of the strength of the second harmonic, B. The parameters used are: $\omega = 0.1, A = 0.1$ and $\phi = 0$.

3.4 *Energy fluctuations over a single period*

Next, we analyse the nature of distribution functions of input energy $P(W_p)$, dissipated heat $P(Q_p)$ and internal energy $P(\Delta U_p)$ for different values of D. These distributions are plotted in figures 8a–8c below resonance ($D = 0.05$), at resonance ($D = 0.12$), and above resonance ($D = 0.3$) respectively. The average internal energy $\langle U \rangle$ being a state function assumes the same value at the beginning and at the end of a period or periods in the time asymptotic regime. Hence total change in the internal energy $\langle \Delta U_p \rangle$ average over a period is equal to zero and it is also expected that the distribution $P(\Delta U_p)$ is symmetric as is evident from figures 8a–8c. The nature of $P(\Delta U_p)$ is explained in [26] for a single harmonic drive. As opposed to

Figure 8. Plots (**a**), (**b**) and (**c**) show the distributions $P(W_p)$, $P(Q_p)$ and $P(\Delta U_p)$ for different values of D, below resonance $D = 0.05$, at resonance $D = 0.12$, and above resonance $D = 0.3$, respectively. Other fixed parameters are also shown on the graphs.
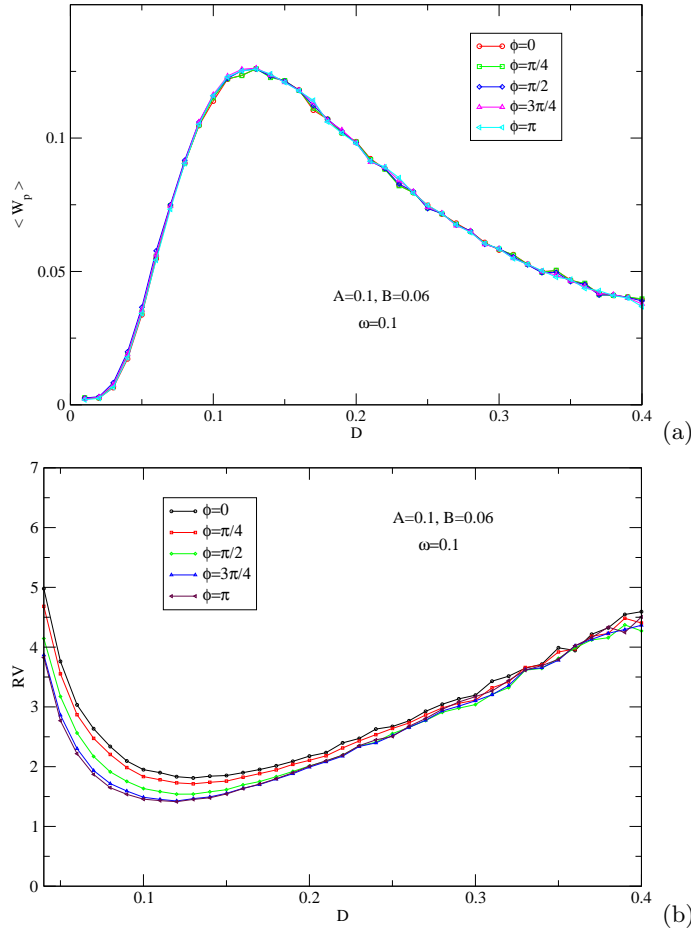
Figure 9. (**a**) The average input energy per period $\langle W_p \rangle$ as a function of D for various values of the phase difference ϕ, (**b**) relative variances (RV) of W_p vs. D. Fixed parameters are shown on the graphs.

ΔU_p, distributions for W_p and Q_p are asymmetric. These distributions keep on changing in shape depending on the number of cycles over which they have been obtained which will be discussed later in connection with steady state fluctuation theorem (SSFT). Probability distributions for work and heat have finite weights for the negative values of their arguments. These negative values correspond to the trajectories where the particle moves against the perturbing AC field over a short time. For small values of D ($D = 0.05$), peak for W_p or Q_p near the origin corresponds mainly to intrawell dynamics of the particle and is mostly confined to a single well. The occasional excursion of the particle into the other well as a function of time is clearly reflected as a small hump at higher values of W_p or Q_p in the plot of $P(W_p)$ and $P(Q_p)$. As we increase D further ($D = 0.12$), interwell dynamics starts playing a dominant role, and hence the distributions become broader. Work
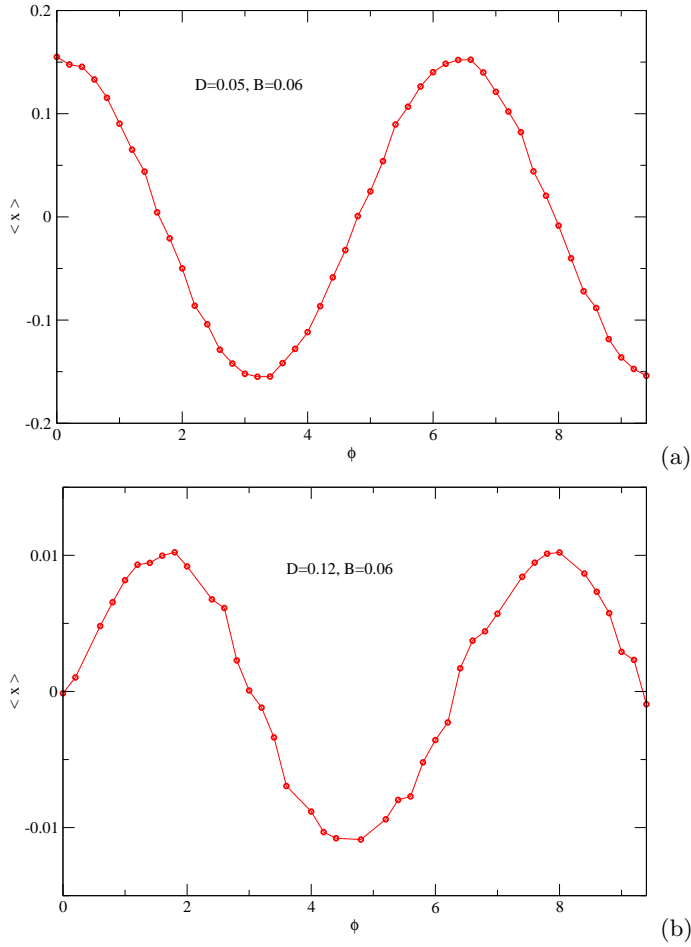
Figure 10. Average position $\langle x \rangle$ as a function of phase ϕ for two different values of D. In (**a**) $D = 0.05$, and in (**b**) $D = 0.12$. Other fixed parameters are: $B = 0.06$, $A = 0.1$ and $\omega = 0.1$.

distribution exhibits three prominent peaks including one at the negative side. For larger values of D beyond SR point, shapes of $P(W_p)$ and $P(Q_p)$ tend closer to Gaussian distribution with increased variance/fluctuations. For such high temperatures, particle makes several random excursions between the two wells during a single time period of the external drive. It may be noted that the relative variances in W_p and Q_p are larger than 1. Also, fluctuations in heat are larger than those of work when averaged over a single period.

3.5 *Effect of phase difference on SR*

We now analyse the role of phase difference (ϕ) between driving fields on pumping and energetics of the system. In figure 9a, we have plotted $\langle W_p \rangle$ as a function
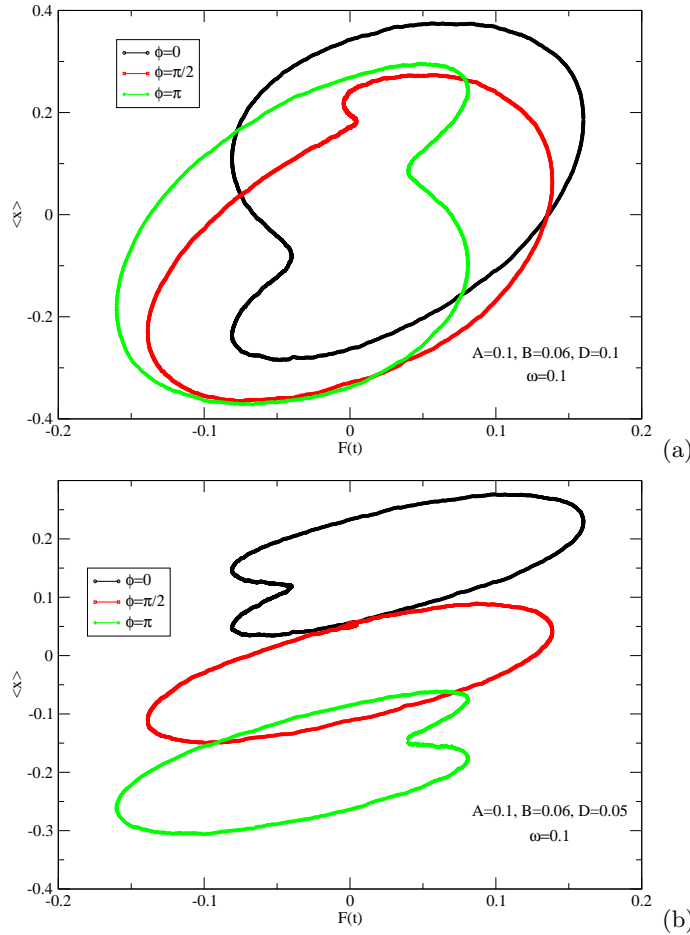
Figure 11. (**a**) Hysteresis loops for different values of ϕ at $D = 0.1$, (**b**) hysteresis loops for different ϕ at $D = 0.05$. Other fixed parameters are: $A = 0.1$, $B = 0.06$ and $\omega = 0.1$

of noise strength D for various values of ϕ. Other physical parameters are held fixed as mentioned in the figure captions. In figure 9b, we have plotted relative variance of W_p as a function of D. It is interesting to note that $\langle W_p \rangle$ is insensitive to ϕ, even though the relative variance depends on ϕ. This is a rather surprising result, given the fact that different values of phase ϕ lead to different degrees of localization of the particle in one of the wells. We have characterized this dynamic localization of particles by average position $\langle x \rangle$ of the particle in the double well potential which in fact can be large depending on D and ϕ. This is shown in figure 10 where we have plotted $\langle x \rangle$ as a function of ϕ for two different values of noise strength D. One can readily see that $\langle x \rangle$ is periodic in ϕ as expected. The insensitivity of $\langle W_p \rangle$ on phase gets reflected in the hysteresis loop areas as shown in figures 11a ($D = 0.1$) and b ($D = 0.05$) for different values of ϕ and a fixed value
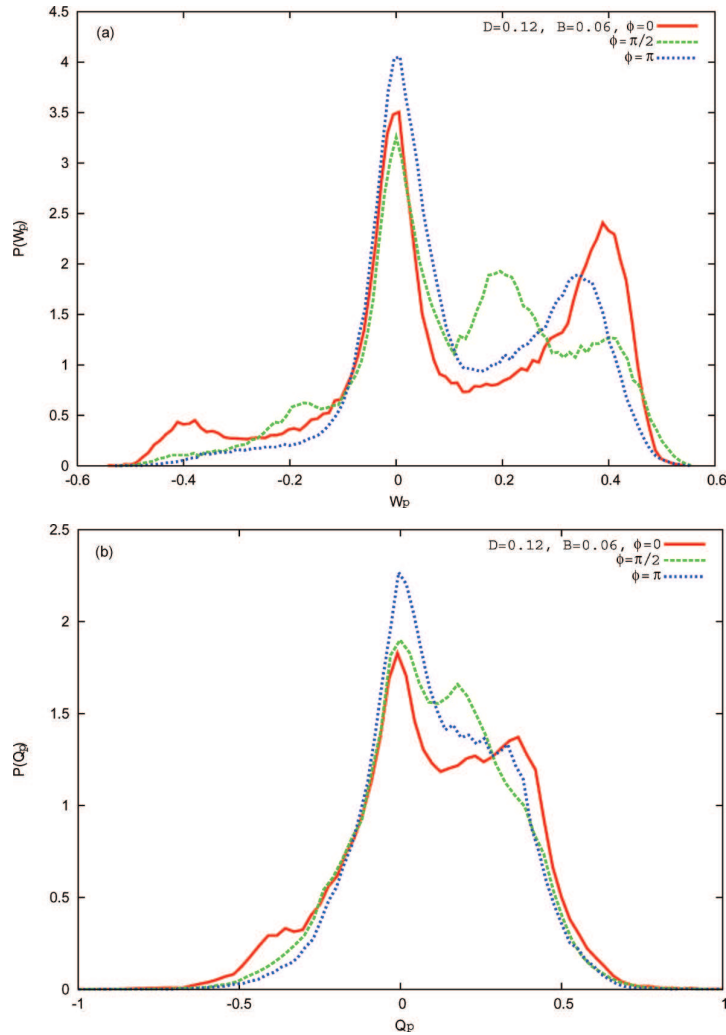
Figure 12. (**a**) and (**b**) show the distributions $P(W_p)$ and $P(Q_p)$ respectively for three different values of ϕ as mentioned on the graphs. Here $D = 0.12$ and $B = 0.06$.

of B ($B = 0.06$). We notice that the areas of the hysteresis loops remain the same for different ϕ. However, their shapes are asymmetric and qualitatively different for different ϕ (i.e., sensitive dependence on phase ϕ). Due to the different degrees of localization or pumping, loops are shifted in $\langle x \rangle$–F plane. The sensitivity of full probability distribution on the phase difference can be seen from figure 12. In these figures we have plotted $P(W_p)$ and $P(Q_p)$ for different values of ϕ as indicated. Note that the distributions exhibit qualitative differences for different ϕ. We have also verified separately that for different values of rocking amplitudes, as long as we are in subthreshold regime, average input energy is not very sensitive to ϕ as
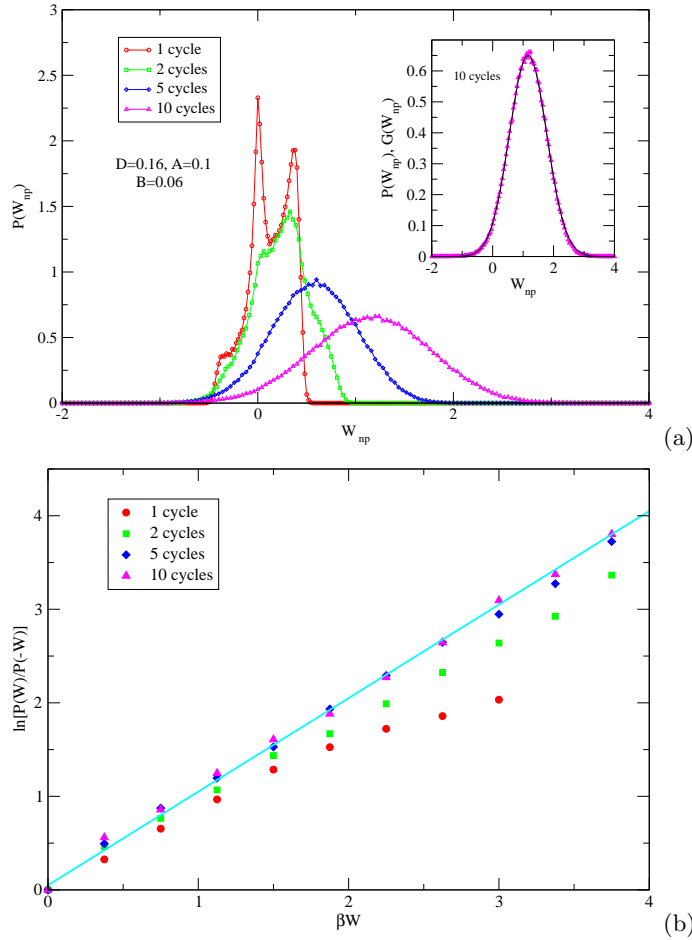
Figure 13. (**a**) The evolution of $P(W_p)$ over different periods. In the inset $P(W_{10p})$ is plotted together with its Gaussian fit $G(W)$. (**b**) The plot of symmetry function ($\ln \frac{P(W)}{P(-W)}$) vs. βW for different periods. The parameters used are: $D = 0.16, \omega = 0.1, B = 0.06, A = 0.1, \phi = 0$. The solid line is the best fit for symmetry function calculated for 10 cycles.

opposed to full probability distribution and hysteresis loops. By tuning ϕ, one can achieve different degrees of particle confinement and can control the fluctuations in heat and work.

3.6 *Energy fluctuations and SSFT*

Finally we discuss the validity of SSFT in the present case of nonequilibrium time periodic steady state. SSFT implies the probability distribution of physical quantity A to satisfy the relation $p(A)/p(-A) = e^{\beta A}$, where β is the inverse temperature of
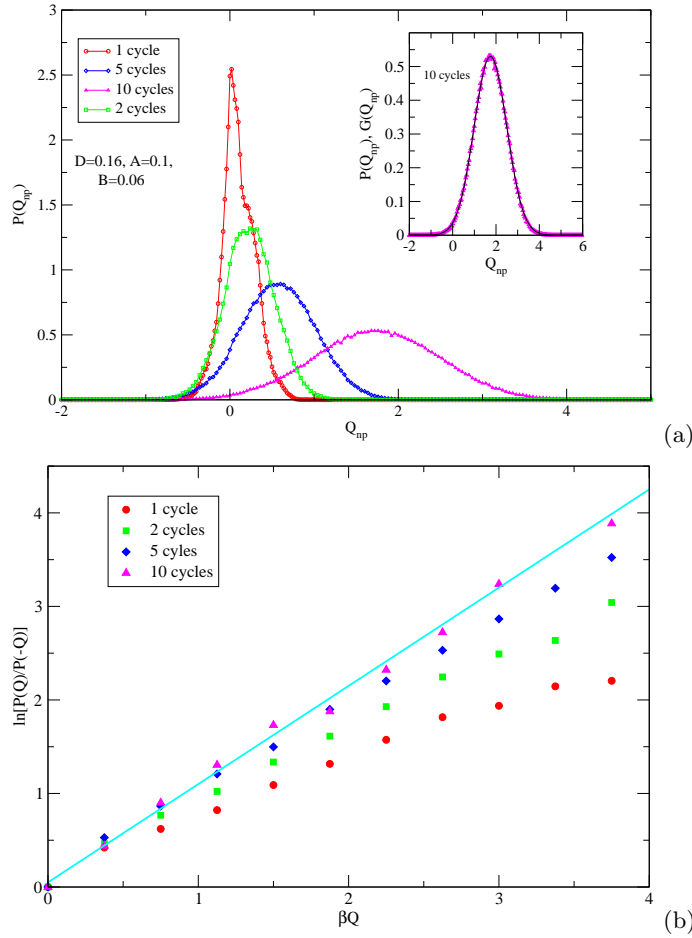
Figure 14. (**a**) The evolution of $P(Q_p)$ over different periods. In the inset $P(Q_{10p})$ is plotted together with its Gaussian fit $G(Q)$. (**b**) The plot of symmetry function ($\ln \frac{P(Q)}{P(-Q)}$) vs. βQ for various values of periods. The solid line is the best fit for symmetry function calculated for 10 cycles. The parameters used are the same as in figure 13.

the bath and A is the work done on the system or the heat released to the bath over a long time of observation. For linear driven systems SSFT for work is indeed satisfied even for work done over a single period in the time asymptotic regime [48]. However, for nonlinear systems, it has been observed experimentally and theoretically that SSFT is satisfied if one considers work done over a large number of cycles [24–26]. In regard to heat, SSFT is known to be valid for $Q < \langle Q \rangle$. Since $\langle Q \rangle$ increases with the number of periods or measured time interval in the limit of large n ($n \to \infty$), $\langle Q \rangle \to \infty$, the conventional SSFT is valid over an entire range of Q [23]. It may be noted that there exists an alternative relation for heat fluctuation, namely, extended heat fluctuation theorem [15,16]. In figure 13 we have plotted

probability distribution $P(W_{np})$ of work W_{np} integrated over different number (n) of periods. $P(W_{np})$ for a single period exhibits double peak structure. As we increase the number of periods the probability distribution shifts towards right as the mean value of work scales linearly with n. Fine structure in probability distributions gets smeared out progressively and distribution tends towards a Gaussian. In the inset of figure 13a we have shown the Gaussian fit for the obtained distribution for 10 cycles. From this fit we obtain $\langle W_{10p} \rangle = 1.16$ and variance $\sigma^2 \equiv \langle W^2 \rangle - \langle W \rangle^2 = 0.37$. From this we can obtain dissipation ratio $R_{\text{diss}} = \frac{\langle W^2 \rangle - \langle W \rangle^2}{2\langle W \rangle/\beta} \simeq 1$, i.e., the variance equals $\frac{2}{\beta}\langle W \rangle$ which is the required condition to satisfy SSFT when observed distribution is Gaussian [24,48,49]. The validity of SSFT for work is also obviously seen from figure 13b where we have plotted the symmetry function ($\ln \frac{P(W)}{P(-W)}$) vs. βW for work evaluated over different cycles as indicated in the figure. As we increase the number of periods from 1 to 10 the slope of symmetry function approaches 1. Hence our data suggest that the SSFT is satisfied even for a finite number of periods. The number of periods above which SSFT is valid depends sensitively on the parameters in the problem.

As already noted, heat fluctuations over a cycle are large compared to work fluctuations. The heat fluctuations get an additional contribution from the internal energy (eq. (4)). Even for a linear problem of harmonic oscillator, heat distribution measured over a single period does not satisfy SSFT as opposed to work fluctuations. The contribution from internal energy is supposed to dominate at very large values of Q, making the distribution $P(Q)$ exponential in the large Q limit [15,16]. However, it may be noted that the distribution of the change in internal energy does not change with the number of periods. Heat being an extensive quantity in time, distribution changes as we change the number of periods as shown in figure 14a where we have plotted $P(Q_{np})$ for various values of n. As anticipated, by increasing n distribution tends towards the Gaussian (see for $n = 10$ cycles). The Gaussian fit for $P(Q_{np})$ (inset of figure 14a) gives the value for the variance as 0.56, and mean as 1.74. Thus dissipation ratio is 0.99, which is closer to unity, satisfying SSFT. In principle, one should be able to observe exponential tails for the distribution $P(Q)$ in the large Q limit [16]. However, our simulations will not be able to detect it due to lack of the required precision. As mentioned earlier, in the limit $n \to \infty$, conventional SSFT holds for heat distributions [26]. In figure 14b, we have plotted the symmetry functions ($\ln \frac{P(Q)}{P(-Q)}$) as a function of βQ. The slope of the symmetry function approaches unity as we increase n, thereby suggesting the validity of SSFT.

4. Conclusion

In conclusion, we have studied the nature of energy fluctuations in a biharmonically driven bistable system. This system is driven simultaneously with two periodic input signals of frequencies ω and 2ω, having phase difference ϕ between them. The presence of additional periodic drive induces particle confinement or localization in a preferred potential well. The degree of confinement analysed in terms of the averaged value of the particle position $\langle x \rangle$ depends on the system parameters. We have shown that in spite of confinement, SR signal when quantified via the averaged

work per period exhibits enhanced response. This is in sharp contrast to the case when confinement is induced by static tilt, which degrades SR. Surprisingly, the average input energy over a period is not very sensitive to ϕ even though variation of ϕ leads to significant particle pumping. However, changes in ϕ does affect qualitatively the nature of hysteresis loop and distributions/fluctuations of work and heat. We have analysed the fluctuations in work done, heat dissipated, and internal energy over a large but finite number of periods. Our data suggest that the SSFT for work and heat holds in this system.

Acknowledgment

References

[1] C Bustamante, J Liphardt and F Ritort, *Phys. Today* **58**, 45 (2005)
[2] D J Evans and D J Searls, *Adv. Phys.* **51**, 1529 (2002)
[3] R J Harris and G M Schütz, *J. Stat. Mech.* p07020 (2007)
[4] F Ritort, *Sem. Poincare* **2**, 63 (2003)
[5] J Kurchan, *J. Stat. Mech.* P07005 (2007)
[6] D J Evans, E G D Cohen and G P Morriss, *Phys. Rev. Lett.* **71**, 2401 (1993); **71**, 3616 (1993) [errata]
[7] D J Evans and D J Searles, *Phys. Rev.* **E50**, 1645 (1994)
[8] G Gallavotti and E G D Cohen, *Phys. Rev. Lett.* **74**, 2694 (1995); *J. Stat. Phys.* **80**, 931 (1995)
[9] J Kurchan, *J. Phys. A: Math. Gen.* **31**, 3719 (1998)
[10] J L Lebowitz and H Spohn, *J. Stat. Phys.* **95**, 333 (1999)
[11] G E Crooks, *Phys. Rev.* **E60**, 2721 (1999)
[12] G E Crooks, *Phys. Rev.* **E61**, 2361 (2000)
[13] U Seifert, *Euro. Phys. J.* **B64**, 423 (2008)
[14] C Jarzynski, *Phys. Rev. Lett.* **78**, 2690 (1997); *Phys. Rev.* **E56**, 5018 (1997)
[15] R van Zon and E G D Cohen, *Phys. Rev.* **E67**, 046102 (2002)
[16] R van Zon and E G D Cohen, *Phys. Rev.* **E69**, 056121 (2004)
[17] O Narayan and A Dhar, *J. Phys. A: Math. Gen.* **37**, 63 (2004)
[18] S Ciliberto and C Laroche, *J. Phys. IV France* **8**, 215 (1998)
[19] G M Wang, E M Sevick, E Mittag, D J Searles and D J Evans, *Phys. Rev. Lett.* **89**, 050601 (2002)
[20] J Liphardt *et al*, *Science* **296**, 1833 (2002)
     F Douarche *et al*, *Europhys. Lett.* **70**, 593 (2005)
     G M Wang *et al*, *Phys. Rev. Lett.* **89**, 050601 (2002)
[21] E M Trepangnier *et al*, *Proc. Natl. Acad. Sci.* **101**, 15038 (2004)
[22] F Douarche, S Joubaud, N B Garnier, A Petrosyan and S Ciliberto, *Phys. Rev. Lett.* **97**, 140603 (2006)
     R von Zon, S Ciliberto and E G D Cohen, *Phys. Rev. Lett.* **92**, 130601 (2004)
[23] S Joubaud, N B Garnier and S Ciliberto, *J. Stat. Mech.* P09018 (2007)
[24] S Saikia, R Roy and A M Jayannavar, *Phys. Lett.* **A369**, 367 (2007)

[25] M Sahoo, S Saikia, M C Mahato and A M Jayannavar, *Physica* **A387**, 6292 (2008)
[26] P Jop, S Ciliberto and A Petrosyan, *Europhys. Lett.* **81**, 50005 (2008)
[27] R Benzi, G Parisi, A Sutera and A Vulpiani, *Tellus* **34**, 10 (1982)
[28] L Gammaitoni, P Hanggi, P Jung and F Marchesoni, *Rev. Mod. Phys.* **70**, 223 (1998)
[29] L Gammaitoni, F Marchesoni and S Santucci, *Phys. Rev. Lett.* **74**, 1052 (1995)
[30] M C Mahato and A M Jayannavar, *Phys. Rev.* **E55**, 6266 (1997)
[31] M C Mahato and A M Jayannavar, *Mod. Phys. Lett.* **B11**, 815 (1997)
[32] M Evstigneev, P Reimann, C Schmitt and C Bechinger, *J. Phys.* **C17**, S3795 (2005)
[33] M C Mahato and A M Jayannavar, *Physica* **A248**, 138 (1998)
[34] T Iwai, *Physica* **A300**, 350 (2001)
[35] D Dan and A M Jayannavar, *Physica* **A345**, 404 (2005)
[36] M Borromeo and F Marchesoni, *Europhys. Lett.* **68**, 783 (2004)
[37] S Savelev *et al*, *Europhys. Lett.* **67**, 179 (2004)
[38] M Borromeo and F Marchesoni, *Phys. Rev.* **E71**, 031105 (2005)
[39] M Borromeo and F Marchesoni, *Acta Phys. Polon.* **B36**, 1421 (2005)
[40] M C Mahato and A M Jayannavar, *Phys. Lett.* **A209**, 21 (1995)
[41] D R Chialvo and M M Millonas, *Phys. Lett.* **A209**, 26 (1995)
[42] A Ajdari, D Mukamel, L Peliti and J Prost, *J. Phys. (Paris)-I* **4**, 1551 (1994)
[43] M Sahoo and A M Jayannavar, cond-mat/arXiv:0905.3901
[44] K Sekimoto, *J. Phys. Soc. Jpn.* **66**, 6335 (1997)
[45] J M R Parrondo and B J De Cisneros, *Appl. Phys. A: Mater. Sci. Process.* **75**, 179 (2002)
[46] H Risken, *The Fokker–Planck equation: Methods of solution and applications* (Springer-Verlag, Berlin, 1989)
[47] R Mannela, *Lecture Notes in Physics* (Springer-Verlag, Berlin, 2000) Vol. 557, p. 353
[48] A M Jayannavar and M Sahoo, *Phys. Rev.* **E75**, 032102 (2007)
[49] M Sahoo and A M Jayannavar, *Pramana – J. Phys.* **70**, 201 (2008)